Combined photoelectron, collision-induced dissociation, and computational studies of parent and fragment anions of N-paranitrophenylsulfonylalanine and N-paranitrophenylalanine

Jason Lambert, Jing Chen, Angela Buonaugurio, Kit H. Bowen, Chi-Linh Do-Thanh, Yilin Wang, Michael D. Best, R. N. Compton, and Thomas Sommerfeld

Citation: The Journal of Chemical Physics **139**, 224308 (2013); doi: 10.1063/1.4834675
View online: http://dx.doi.org/10.1063/1.4834675
View Table of Contents: http://scitation.aip.org/content/aip/journal/jcp/139/22?ver=pdfcov
Published by the AIP Publishing

Combined photoelectron, collision-induced dissociation, and computational studies of parent and fragment anions of *N*-paranitrophenylsulfonylalanine and *N*-paranitrophenylalanine

Jason Lambert,[1] Jing Chen,[2] Angela Buonaugurio,[2] Kit H. Bowen,[2,a)] Chi-Linh Do-Thanh,[3] Yilin Wang,[3] Michael D. Best,[3] R. N. Compton,[1,3,a)] and Thomas Sommerfeld[4]
[1]*Department of Physics and Astronomy, University of Tennessee, Knoxville, Tennessee 37996, USA*
[2]*Department of Chemistry, Johns Hopkins University, Baltimore, Maryland 21218, USA*
[3]*Department of Chemistry, University of Tennessee, Knoxville, Tennessee 37996, USA*
[4]*Department of Chemistry and Physics, Southeastern Louisiana University, Hammond, Louisiana 70402, USA*

(Received 9 July 2013; accepted 12 November 2013; published online 12 December 2013)

After synthesizing the compounds *N*-paranitrophenylsulfonylalanine (NPNPSA) and *N*-paranitrophenylalanine (NPNPA), the photoelectron spectrum of the valence anion of *N*-paranitrophenylsulfonylalanine $(NPNPSA)^-$, was measured and the collision-induced dissociation (CID) pathways of deprotonated *N*-paranitrophenylsulfonylalanine $(NPNPSA\text{-}H)^-$ and deprotonated *N*-paranitrophenylalanine $(NPNPA\text{-}H)^-$ were determined. Pertinent calculations were conducted to analyze both sets of experimental data. From the valence anion photoelectron spectrum of $(NPNPSA)^-$, the adiabatic electron affinity (AEA) of NPNPSA was determined to be 1.7 ± 0.1 eV, while the vertical detachment energy (VDE) of $(NPNPSA)^-$ was found to be 2.3 ± 0.1 eV. Calculations for four low lying conformers of $(NPNPSA)^-$ gave AEA values in the range of 1.6–2.1 eV and VDE values in the range of 2.0–2.4 eV. These calculations are in very good agreement with the experimental values. While the NPNPA anion $(NPNPSA)^-$ was not observed experimentally it was studied computationally. The six low lying $(NPNPSA)^-$ conformers were identified and calculated to have AEA values in the range of 0.7–1.2 eV and VDE values in the range of 0.9–1.6 eV. CID was used to study the fragmentation patterns of deprotonated NPNPA and deprotonated NPNPSA. Based on the CID data and calculations, the excess charge was located on the delocalized π-orbitals of the nitrobenzene moiety. This is made evident by the fact that the dominant fragments all contained the nitrobenzene moiety even though the parent anions used for the CID study were formed via deprotonation of the carboxylic acid. The dipole-bound anions of both molecules are studied theoretically using the results of previous studies on nitrobenzene as a reference. [http://dx.doi.org/10.1063/1.4834675]

I. INTRODUCTION

Synthesized amino acid derivatives have become especially important in many areas of molecular biology where they often act as protein markers.[2] While addition of these unnatural amino acids to proteins has become routine procedure in site-specific functionality,[3–5] the properties of such complex systems need to be characterized for them to be useful. One method is to examine the influence of well-characterized properties of the smaller moieties on the extended molecular complex. A recent theoretical study has explored this concept of a "molecule-in-molecule (MIM) approach."[6]

Within the past two decades, new experimental and theoretical methods have been developed to examine the properties of complex molecules and their ions in the gas phase. The conformational flexibility and fragility of these extended molecules require gentle heating into the gas phase for meaningful studies of photoelectron spectroscopy (PES) of their intact parent anions and the determination of electron affinities. Likewise, electrospray ionization also allows the preparation of molecular anions, albeit the ions are often formed via deprotonation, for study by collision induced dissociation (CID). Under well-controlled conditions, this method can provide direct information on the fragmentation pathways and, under proper conditions, can provide estimates of the energy required to break molecular bonds of interest.

Herein, we employ both PES and CID techniques to study the negative ion properties of two newly synthesized amino acid derivatives. *N*-paranitrophenylsulfonylalanine (NPNPSA) and *N*-paranitrophenylalanine (NPNPA) were synthesized and both (*S*)- and (*R*)-enantiomers studied as a check of experimental reproducibility. These complex molecules contain nitrobenzene, sulfur dioxide, and alanine, all of which have had their negative ion properties well characterized. We present a combination of experiment and theory to examine how the negative ion properties of the individual components can be correlated to better characterize the negative ion properties of these newly synthesized amino acids.

[a)]Authors to whom correspondence should be addressed. Electronic addresses: rcompton@utk.edu and kbowen@jhu.edu.

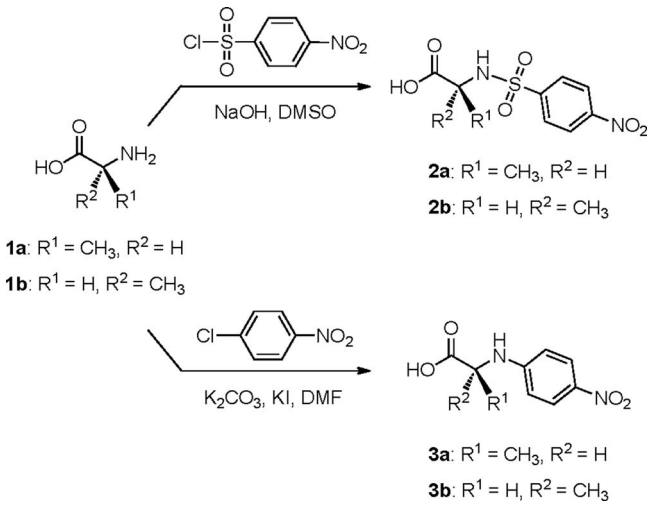

FIG. 1. Preparation scheme of (*S*)-NPNPSA (**2a**), (*R*)-NPNPSA (**2b**), (*S*)-NPNPA (**3a**), and (*R*)-NPNPA (**3b**).

II. SAMPLE PREPARATION

A. Preparation of (*S*)-NPNPSA (2a) and (*R*)-NPNPSA (2b)

The synthesis of (*S*)-NPNPSA (**2a**, see Figure 1) was performed by adding 1 M of sodium hydroxide solution (5 ml) to (*S*)-alanine (**1a**, 0.21 g, 2.40 mmol) and cooled to 0 °C. Then 4-nitrobenzenesulfonyl chloride (0.82 g, 3.61 mmol) was added in small portions to the reaction mixture and was stirred at room temperature overnight, followed by rinsing with ethyl acetate (20 ml). The aqueous layer was then acidified with 1 M hydrochloric acid (10 ml) and extracted with ethyl acetate (15 ml). The resultant organic layer was dried with magnesium sulfate, filtered, and concentrated. Column chromatography over silica gel with gradient elution from 5%–20% methanol/dichloromethane gave the product **2a** as a yellow solid (0.29 g, 44%). Its enantiomer (*R*)-NPNPSA (**2b**) was similarly prepared using (*R*)-alanine (**1b**, 0.23 g, 2.58 mmol), 1 M sodium hydroxide (7 ml) and 4-nitrobenzenesulfonyl chloride (0.87 g, 3.86 mmol), which yielded **2b** as a white solid (0.24 g, 35%). The characterization using Nuclear Magnetic Resonance (NMR) [^{1}H NMR (300 MHz, DMSO (dimethyl sulfoxide)-d_6) δ 8.37 (d, $J = 7.1$ Hz, 2H), 8.04 (d, $J = 7.1$ Hz, 2H), 3.68 (q, $J = 7.1$ Hz, 1H), 1.19 (d, $J = 7.1$ Hz, 3H)] match those reported in the literature.[7,8]

B. Preparation of (*S*)-NPNPA (3a) and (*R*)-NPNPA (3b)

(*S*)-NPNPA (**3a**, see Figure 1) was synthesized by first adding 20 ml of *N,N*-dimethylformamide (DMF) to (*S*)-alanine (**1a**, 0.95 g, 10.7 mmol). Potassium carbonate (2.95 g, 21.3 mmol) and potassium iodide (1.77 g, 10.7 mmol) were then added to the stirring solution. 4-Chloronitrobenzene (3.36 g, 21.3 mmol) was added in small portions, and the reaction mixture was stirred and refluxed at 120 °C overnight. The solvent was removed via rotary evaporation. The crude product was then dissolved in 50 ml of water, acidified with 1 M hydrochloric acid (20 ml), and extracted with ethyl acetate (50 ml). The resultant organic layer was dried with magnesium sulfate, filtered, and concentrated. Column chromatography over silica gel with gradient elution from 1%–25% methanol/dichloromethane gave the product as a yellow solid (1.21 g, 54%). Enantiomer **3b** was similarly prepared using (*R*)-alanine (**1b,** 0.88 g, 9.90 mmol), 20 ml of DMF, potassium carbonate (2.74 g, 19.8 mmol), tetrabutylammonium iodide (3.66 g, 9.90 mmol), and 4-chloronitrobenzene (3.12 g, 19.8 mmol), which yielded **3b** as a yellow solid (0.67 g, 32%). The characterization using NMR [^{1}H NMR (300 MHz, CD_3OD) δ 8.02 (d, 2H, $J = 9$ Hz), 6.60 (d, 2H, $J = 9$ Hz), 3.96 (q, 1H, $J = 9$ Hz), 1.48 (d, 3H, $J = 9$ Hz)] match those reported in the literature.[9]

III. EXPERIMENTAL AND COMPUTATIONAL METHODS

A. Photoelectron spectroscopy

Negative ion PES was conducted by crossing a mass-selected beam of parent negative ions with a fixed-frequency photon beam and energy-analyzing the resultant photodetached electrons. The photodetachment process is governed by the relationship $h\nu = EBE + EKE$, where $h\nu$ is the photon energy, electron binding energy (EBE) is the electron binding energy, i.e., the transition energy between the anion and a particular vibrational state of its neutral counterpart, and EKE is the electron kinetic energy.

The parent negative ions were formed in a supersonic expansion nozzle-ion source. Each synthesized enantiomer sample was placed in the stagnation chamber of the source, heated up to 100 °C–130 °C, and co-expanded with ~3–4 atm of argon gas through a 15 μm orifice into $\sim 10^{-4}$ Torr vacuum. Negative ions were then formed by injecting low energy electrons from a hot and even more negatively biased, thoriated iridium filament into the expanding jet where the microplasma was formed in the presence of a weak external magnetic field. The anions were extracted and transported via a series of ion optics through the flight tube of a 90° magnetic sector mass spectrometer with a typical mass resolution ($m/\Delta m$) of ~400. The mass-selected anions of interest were then crossed with an intracavity operated argon ion laser beam, and the resultant photodetached electrons were energy-analyzed in a hemispherical electron energy analyzer with a resolution of ~30 meV. The photoelectron spectra reported herein were recorded with 2.54 eV photons and calibrated against the well-known photoelectron spectrum of the O^- anion.[10]

B. Collision induced dissociation

Because (*R*)- and (*S*)- are chiral designations and our experiment does not distinguish between enantiomers, the results of both enantiomers are expected be identical, therefore only CID of the (*S*)- enantiomer is presented. Deprotonated NPNPA and NPNPSA were produced using an electrospray ionization (TurboIonSpray®) source. Solutions of (*S*)-NPNPSA and (*S*)-NPNPA were prepared at a concentration of 200 μg/ml in a 1:1 HPLC grade water and methanol mixture and then passed through a 0.005 in. inlet syringe tip

with a flow rate of 5 to 20 μl/min. The temperature of the source was set to 100 °C, and the ion spray bias voltage was optimized empirically for each CID spectrum to give the highest deprotonated parent signal intensity.

Collision induced dissociation was performed using an Applied Biosystems Q-Star Elite triple quadrupole mass spectrometer (MS) and is outlined in the paper by Smith *et al.*[11] Ions were formed by electrospray ionization and the mass selection and CID were performed in an initial quadrupole MS followed by introduction into the collision region. The ions resulting from the collision region were then analyzed by a reflectron time-of-flight MS. The signals of all ions at each energy reported in the CID spectra were averaged for 30 s. Argon was used as the collision gas for all reported experiments. The energy scale was determined using the collision induced dissociation process $I_3^- \rightarrow I_2 + I^-$ (see Ref. 11 for details). The lab frame energy step-size for deprotonated (*S*)-NPNPSA was 0.25 eV and 0.5 eV for deprotonated (*S*)-NPNPA. The energy calibration was further estimated by using a retardation analysis, which was in agreement with the $I_3^- \rightarrow I_2 + I^-$ analysis.[11]

It was found that the observed thresholds for the CID secondary ions shifted slightly to lower energy as the argon collision gas pressure increased. Although the energy shifts with pressure are small (~0.2 eV in the center of mass), we conclude that multiple ions collisions with the argon gas were adding internal energy into the large and flexible anions, which shows up as internal vibrational heating of the anion leading to a lower threshold. As a result we only present approximate ion dissociation energies. The dissociation energy was estimated by extrapolating the linear portion of the CID spectrum for each channel to zero intensity. Because the linear extrapolation will overestimate the dissociation energy and multiple collisions lower the estimated dissociation energy there is some cancellation of error but the extent of this cancellation is unknown.

C. Computational methods

Computational investigations focused on characterizing both valence and dipole-bound states of the NPNPSA and NPNPA anions. These molecules are too large to use reliable *ab initio* methods typically required for accurately predicting electron affinities so more approximate methods must be employed. This section reports all computational methods employed in detail, however, the full justification for selecting these methods is provided in the supplementary material.[33]

Three basis sets were employed, Dunning's correlation consistent double-ζ (aug-cc-pVDZ) and triple-ζ (aug-cc-pVTZ) sets,[12,13] and Ahlrichs's redefined triple-ζ set augmented with a minimal set of diffuse functions (ma-Def2-TZVP).[14,15] For computing dipole-bound states an additional 6*s*6*p*5*d* set of diffuse functions was centered at the center-of-mass of the molecule (even-tempered exponents, smallest exponent 0.02 for all angular momenta, even-scaling factor $\sqrt{10}$). For consistency, all geometry optimizations of neutral and negatively charged conformers of nitrobenzene, NPNPSA, and NPNPA were carried out using the same method, the M06-2X hybrid functional[16] and the aug-cc-pVDZ basis set. The progression of *ab initio* methods, self-consistent field (SCF) calculations, second-order Moeller-Plesset perturbation theory (MP2), coupled-cluster calculations with single and double substitutions (CCSD), CCSD with a perturbative estimate of triple substitutions (CCSD(T)) was used for the nitrobenzene reference system, and its electron binding energies were also computed directly with the equation-of-motion couple-cluster method for electron affinities (EOM-CCSD) and the equation-of-motion MP2 method (EOM-MP2).[17,18] In the MP2 and the coupled-cluster calculations, all core electrons were frozen in their SCF orbitals. Moreover, for the open-shell valence state of the nitrobenzene anion, CCSD calculations were started from three sets of orbitals, unrestricted (UHF) and restricted (ROHF) SCF orbitals of the anion as well as from an anion-like occupation of the SCF orbitals of the respective neutral (QRHF). Electron binding energies were also computed using the following density functionals, the generalized-gradient-approximation (GGA) functionals BLYP, BP86, PBE, and OLYP, the meta-GGA functional TPSS, and the hybrid functionals M06-2X, B3LYP, and O3LYP.[16,19–24] Three program packages were employed: Gaussian09[25] for M06-2X calculations, Orca[26] for all other density functional and some of the MP2 calculations, and CFOUR[27] for MP2 and all coupled-cluster calculations.

Computing reliable electron affinities is in general a challenging task, and the present case is particularly difficult, because spin-contamination in the UHF wavefunction of the valence anion makes MP2 for these states effectively useless. Therefore, the only reasonable choice for predicting adiabatic attachment and vertical detachment energies in this context is to calibrate a density functional method with a reference system. Since the valence states of the NPNPSA and NPNPA anions are both well described by an excess electron occupying the nitrobenzene moiety of these larger species, a number of density functionals were tested using the well-characterized $^2B_1$ valence state of nitrobenzene as a basis of comparison. The details of these calculations are described in the supplementary material (see in particular Table S1).[33] The main conclusion regarding electron binding energies of nitrobenzene-like anions is that the best option out of the eight functionals tested is the GGA OLYP or the meta GGA TPSS with a triple-ζ basis sets such as the ma-Def2-TZVP set. We expect that with this type of approach the AEA of any NPNPSA or NPNPA conformer should be well reproduced within one or two tenths of an eV, while vertical detachment energy (VDEs) and Vertical Electron Affinities (VEA) are somewhat more sensitive and are expected to be overestimated by a few tenths of an eV.

Computing dipole-bound states is even more challenging because standard density functional methods at the present time cannot be used.[33] For the NPNPA conformers the usual sequence of Koopmans's Theorem (KT), ΔSCF, and ΔMP2 can be used, because for the dipole-bound states spin-contamination is negligible. Estimation of higher order correlation effects is based on comparison with the nitrobenzene reference system (see Table S2 of the supplementary material).[33] For most conformers of NPNPSA, on the other

hand, the valence states of the anion are already very low in energy, mix with the dipole-bound states, and none of the states resulting from vertical attachment can be characterized as purely dipole-bound or purely valence. Thus, for NPNPSA only a single conformer is discussed below.

IV. RESULTS AND DISCUSSION

A. PES

Attempts were first directed to produce the dipole-bound anions of these systems. The dipole moments of NPNPSA and NPNPA were calculated to be 4.5 D and 7.6 D, respectively.[33] These values are well above both the theoretical critical value for a point dipole of 1.625 D and the empirical minimum value of 2.5 D necessary to support a stable dipole-bound state. Thus, it is believed that dipole-bound anions might be produced, however, slow free electron attachment to a polar molecule to form dipole-bound anions is unlikely. There is no mechanism for stabilization without a third body. Evidence of a dipole-bound anion is characterized in the photoelectron spectrum as a single, narrow peak close to zero EBE. The near zero EBE is indicative of the nearly identical geometries between the anion and neutral. However, as was also the case in the photoelectron spectrum of nitrobenzene,[1] only the valence anions were observed. We postulate that, as in the case of nitrobenzene, the dipole-bound anions will act as a "doorway state" to the more stable valence anions.

The photoelectron spectra of the valence (*S*)- and (*R*)-NPNPSA anions are shown in Figure 2. As expected, both enantiomer anions exhibit very similar photoelectron spectral profiles. Each photoelectron spectrum has a maximum EBE value at 2.3 eV and a threshold EBE value at ∼1.7 eV. Thus, the VDEs of both (*S*)- and (*R*)-NPNPSA anions are assigned at 2.3 ± 0.1 eV. Based on the location of the threshold and typical patterns of anion photoelectron spectral profiles, the AEA values are assigned as lying in the vicinity of 1.7 ± 0.1 eV, with vibrational hot bands accounting for the first 0.1–0.2 eV of the low EBE tail. Due to the Franck-Condon factors and large degrees of freedom for these anions, any vibrational structures in both spectra remain unresolved.

Surprisingly, after much searching, we were unable to produce parent anions of (*S*)- and (*R*)-NPNPA in the gas phase. A possible explanation is that the cross section for electron attachment to NPNPA is too small to be produced by slow electron attachment or that dissociation or autodetachment occurs more readily before our detection time scale (∼10 μs). Gas phase electron attachment studies of this molecule using well-controlled electron beams could prove interesting.

B. CID

The secondary ion mass spectra of deprotonated (*S*)-NPNPSA (NPNPSA-H)$^-$ and deprotonated (*S*)-NPNPA (NPNPA-H)$^-$ following collision induced dissociation are shown in Figure 3. The measured CID spectra using argon as the collision gas as function of the center-of-mass collision energy are shown in the supplementary material.[33] Figures 4 and 5 give the estimated cross-section for each channel of (NPNPSA-H)$^-$ and (NPNPA-H)$^-$. Extrapolations of the linear region of the cross-section to zero intensity provide the estimate of the dissociation energy.

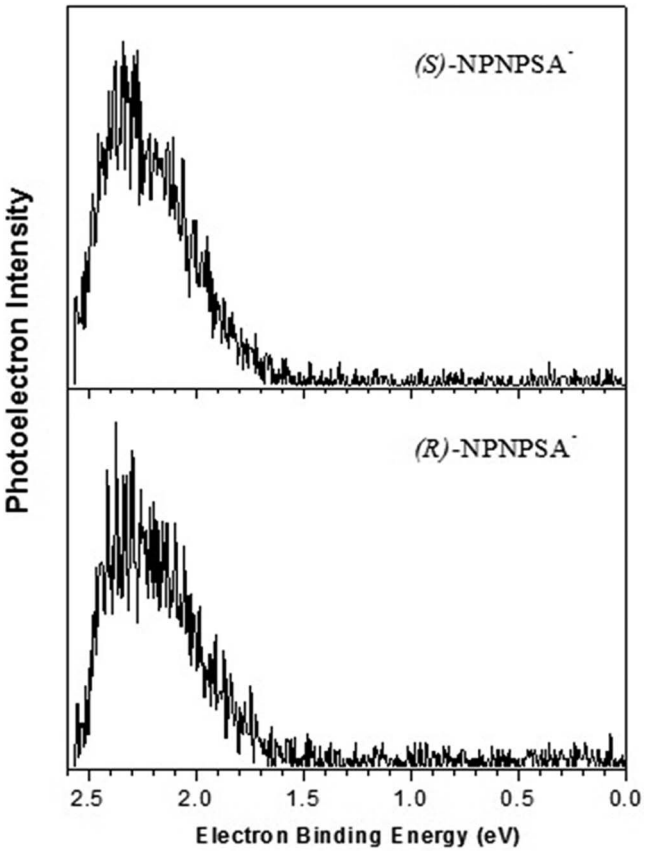

FIG. 2. Photoelectron spectra of (*S*)- and (*R*)- NPNPSA valence anions recorded with 2.54 eV photons.

The primary fragments of (NPNPSA-H)$^-$ (273 amu) upon collisions with argon and the major pathways yielding these fragments are illustrated in Figure 6, and the predicted changes of the Gibbs free energy and the enthalpy are given in Table S8 of the supplementary material.[33] The fragment *m*/*z* 201 anion is formed when the bond between the stereocenter of alanine and the amino nitrogen break. The *m*/*z* 186 anion is formed when the bond between the nitrogen and the sulfur breaks. We predict that the neutral 87 amu counterpart of the *m*/*z* 186 anion autodissociates into acetaldimine[28] and CO_2 by breaking the bond between the alanine stereocenter and CO_2.

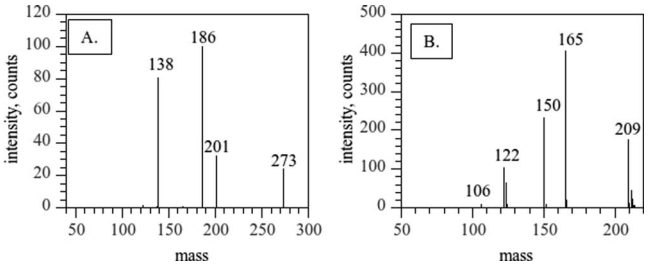

FIG. 3. (a) The mass spectrum of (*S*)-(NPNPSA–H)$^-$ after CID and (b) the mass spectrum of (*S*)-(NPNPA–H)$^-$ after CID. The pathways corresponding to (a) and (b) are illustrated in Figures 4 and 5, respectively.

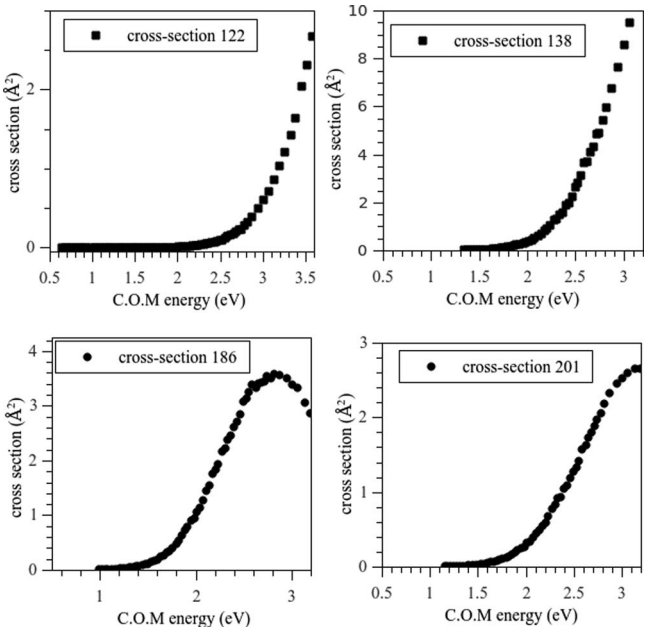

FIG. 4. The estimated cross-section for each dissociation path of $(NPNPSA–H)^-$.

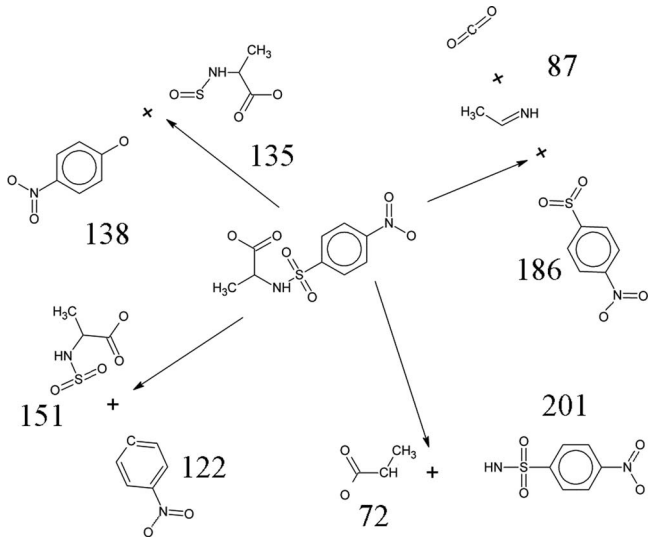

FIG. 6. Collision induced dissociation pathways for $(NPNPSA–H)^-$.

This is supported by geometry optimization calculations using B3LYP/aug-cc-pVDZ of the 87 amu fragment. Figure S3 of the supplementary material shows the final structure reached by optimization of this fragment, which is relevant to both deprotonated NPNPSA and deprotonated NPNPA.[33] The estimated dissociation energy for each channel of deprotonated NPNPSA is given in Table I.

The pathway leading to the *m/z* 138 anion is attributed to the bonding of an oxygen atom to nitrobenzene in place of the sulfur at the para-position, forming a deprotonated nitrophenol. This requires a rearrangement reaction and is supported from geometry optimizations using B3LYP/aug-cc-pVDZ of the assumed *m/z* 138 anion and the neutral 135 amu counterpart of this dissociation pathway.[33] This rearrangement reaction involving the loss of SO_2 is not unprecedented. Wang *et al.*[29] observed a similar rearrangement reaction for a biologically derived sulfonamide $\beta 3$ agonist, although they reported only the loss of SO_2. This differs in the experiments reported here because the oxygen atom is proposed to be scavenged from SO_2. Finally, the final pathway resulting in the *m/z* 122 anion observed corresponds to the nitrobenzene anion minus a hydrogen atom.

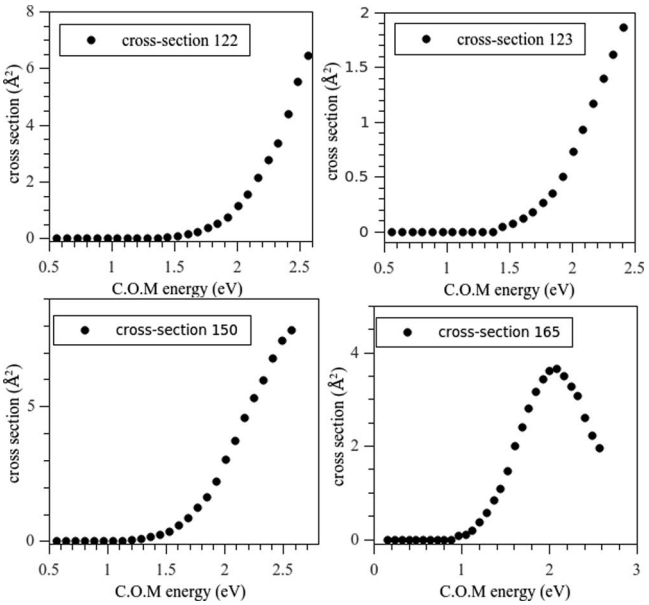

FIG. 5. The estimated cross-section for each dissociation pathway $(NPNPA–H)^-$.

The primary fragments of $(NPNPA-H)^-$ (209 amu) upon collisions with argon along with the major pathways yielding these fragments are illustrated in Figure 7. The predicted changes of the Gibbs free energy and the enthalpy are given in Table S9 of the supplementary material.[33] The pathway producing the *m/z* 165 anion results from the loss of CO_2. We believe the *m/z* 150 anion results from the loss of both CO_2 and NH, then couple forming the neutral fragment counterpart. This requires a rearrangement reaction where the alanine stereocenter attaches to the para-position of the nitrobenzene, and produces an anion that satisfies the "even electron rule."[30,31] The pathway producing the *m/z* 123 anion (nitrobenzene) and the last pathway producing the *m/z* 122 anion (deprotonated nitrobenzene) have similar thresholds, however the deprotonated nitrobenzene anion

TABLE I. The estimated dissociation energies (DE) of deprotonated NPNPSA.

m/z	DE (eV)
201	2.01 ± 0.3
186	1.68 ± 0.3
138	2.42 ± 0.3
122	3.08 ± 0.3

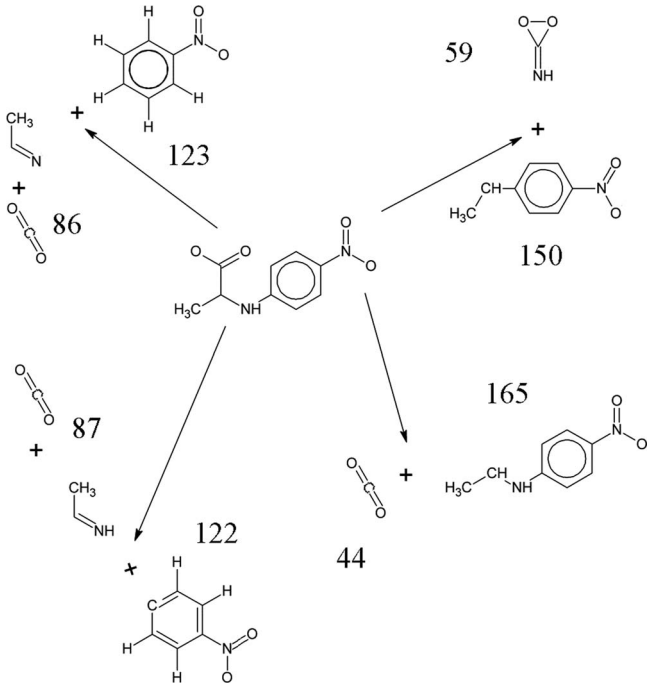

FIG. 7. Collision induced dissociation pathways of $(NPNPA–H)^-$.

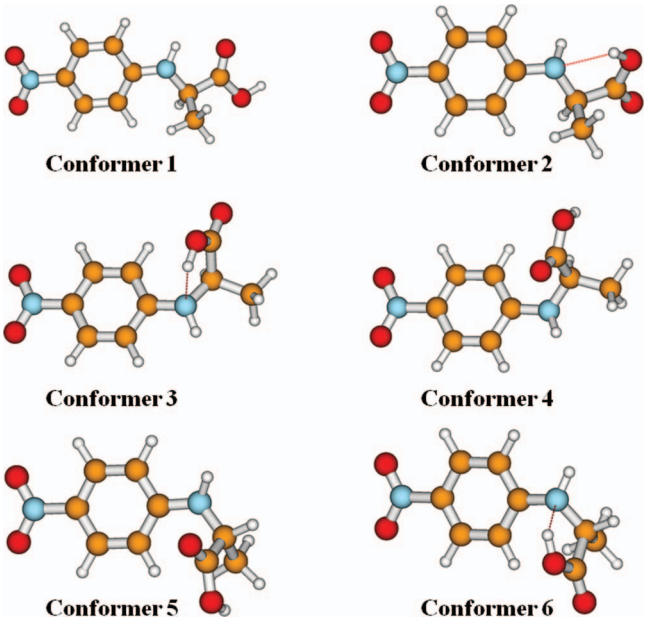

FIG. 8. The six low energy conformers of neutral NPNPA.

dominates. The remaining smaller fragments at 106 amu are attributed to the loss of oxygen from the deprotonated nitrobenzene. Likewise, the 92 amu anion is attributed to deprotonated phenol and the 46 amu anion is attributed to NO_2^-. Unfortunately, these mass fragments had extremely low abundance in the CID spectrum preventing an estimation of these dissociation energies. The estimated dissociation energy for each channel of deprotonated NPNPA is given in Table II.

The fragmentation pathways of $(NPNPSA-H)^-$ and $(NPNPA-H)^-$ revealed that all the anions were formed through deprotonation of the carboxylic acid, yet the charge was always found on the delocalized π orbitals of the nitrobenzene. An exception applies to the very weak case of the NO_2^-anion. The delocalized orbitals stabilized the negative ion by reducing the repulsive columbic interactions. This was evident from the observation that the nitrobenzene unit appeared in all the fragment anions produced in these experiments, along with the fact that the NO_2^- anion was only observed at very low intensities in the NPNPA spectrum. Finally, because the lifetime of CO_2^- is 22–60 μs depending on its internal energy,[32] we cannot rule out the possibility that the metastable CO_2^-(m/z 44) is formed and then decays before the ion can be detected.

TABLE II. The estimated dissociation energies (DE) values of NPNPA.

m/z	DE (eV)
165	1.2 ± 0.3
150	1.6 ± 0.3
123	1.7 ± 0.3
122	1.9 ± 0.3

C. Computational results

This section investigates the negative ion properties of individual NPNPSA and NPNPA conformers. Both molecules have conformational flexibility regarding the single bonds of the alanine side-chain, and NPNPSA has additional flexibility regarding the N-S and the C-S bonds. Consequently, one may expect several conformers to be thermally accessible at room temperature, and many experimental observations will be averages of conformer populations. A manual conformer search for NPNPA yielded six distinct minimal energy structures shown in Figure 8 and four distinct minimal energy structures for NPNPSA shown in Figure 9. The relative energies computed for these conformers using the M06-2X density functional and the MP2 method with the aug-cc-pVDZ basis set are listed in Tables S3 and S4 of the supplementary material.[33] The MP2 method predicts somewhat smaller energy gaps between the conformers and since the relevant differences between the conformers are mostly intermolecular-like

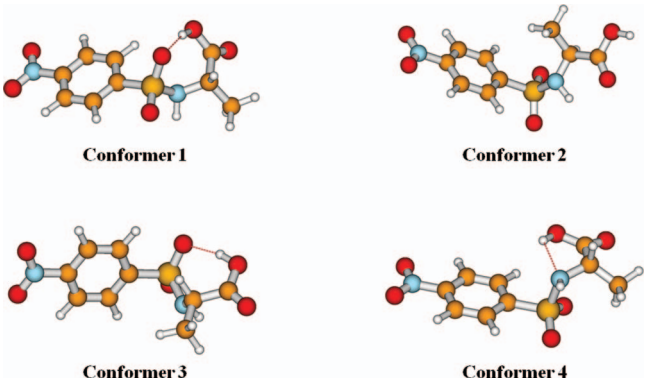

FIG. 9. The four low energy conformers of neutral NPNPSA.

contacts, such as hydrogen bonds and hydrogen-π interactions, the MP2 results are probably more reliable. Nonetheless, the predicted energetic order is identical, and the same is true for the overall qualitative picture.

Both methods predict that for both neutral molecules the "stretched-out" conformers without any intermolecular-like contacts are most stable; however, there are two or three other conformers within about 20 kJ/mol. All of these conformers can attach electrons into dipole-bound or in valence states. However, in contrast to nitrobenzene, where these two types of states are cleanly separated by symmetry, the negative ion states for NPNPA and especially for NPNPSA are often of mixed character, similar to that found for para-nitroaniline.[11] Dipole-bound states of NPNPSA and NPNPA are intrinsically fascinating, because of the interplay between the part of the molecule acting as a local dipole and other parts acting essentially as an excluded volume, which puts the MIM hypothesis to a test. Moreover, dipole-bound states have been shown to provide efficient "doorways" for attachment of low-energy (thermal) electrons into the valence orbitals, and represent therefore in many contexts an early intermediate in electron-induced reactions. Similar to other short-lived intermediates direct experimental observation can be challenging, and at least for the time being we can only report a theoretical characterization.

Regarding accurate characterization of dipole-bound states, most conformers of both the NPNPSA and NPNPA anions unfortunately require methods that we cannot apply due to the size of these molecules. Two major obstacles exist; first, the standard density functional methods cannot yet be applied to electronic states with diffuse densities and second for most NPNPSA conformers the dipole-bound state is very close in energy to the valence state. This not only makes unraveling these two states a formidable challenge but also adds the practical problem of achieving SCF convergence on the "right" state. Nevertheless, the relevant trends can be identified by making careful comparison to the reference system, nitrobenzene, as outlined in the supplementary material.[33]

All low-energy conformers of NPNPA show substantial dipole moments in excess of 6 D (conformer 2, which has an energy of 30 kJ/mol above the most stable neutral conformer, has a somewhat smaller dipole moment; see Table S7 of the supplementary material)[33]. Because the NPNPA conformers are far more polar than nitrobenzene and their VEAs are accordingly larger, higher order electron-correlation corrections may be expected to be less important than for nitrobenzene. Therefore, the ΔMP2 values listed in the supplementary material[33] (40–140 meV; Table S7) are probably reasonable predictions by themselves. Further corrections for both more complete basis sets and higher order correlation effects are expected to yield larger VEAs. Finally, nitrobenzene and other organic molecules can serve as guiding examples and these corrections may be expected to be somewhere in the 10%–20% range.

There are some interesting differences between the conformers in the sense that despite similar, fairly large dipole moments, the predicted VEAs of different conformers differ by as much as a factor of three. These differences can be explained by different interactions between local bond-moments and excluded volume effects. The essential local dipole-moments stem from the NO_2 group and from the carbonyl group, whereas the phenyl ring acts as an excluded volume, that is, a region where the attractive potential due to the NO_2 group may be strong, but the repulsive potential due to Pauli repulsion with the valence electrons of the phenyl ring is even stronger. The relative orientation of these three groups is such that the excess electron can be closer to both local dipoles, which have the large electron binding energies and consequently a more compact distribution of the excess electron, in those conformers.

For NPNPSA it was only possible to identify the dipole-bound state of conformer 2.[33] At the equilibrium structures of all other conformers the mixing between valence and dipole-bound states is too strong, and a VEA associated with a "pure" dipole-bound state cannot be assigned. Conformer 2 of NPNPSA is predicted to have a dipole moment of 4.5 D, and its VEA is predicted to be 20 meV using the MP2 method, which is roughly twice the VEA predicted for nitrobenzene with the same method. Again, using nitrobenzene as a guide, one may expect this conformer to have a dipole-bound state with a VEA of about 30 meV. Moreover, owing to the strong mixing of dipole-bound and valence states for most NPNPSA conformers, one may expect the doorway mechanism for this species to be efficient.

In addition to the dipole-bound states, all NPNPSA and NPNPA conformers are found to support bound valence states. Similar to the $^2B_1$ valence state of nitrobenzene the attached electron occupies a π^*-like orbital of the nitrobenzene moiety, and there is only a modest change in the bond lengths and bond angles of the nitrobenzene unit. What changes more dramatically are the torsion angles, in particular for those conformers with hydrogen bonds pointing in the direction of the phenyl ring and closely related with these structural changes there is a change in the energetic order upon electron attachment.

For the NPNPA anion the three conformers, shown in Figure 10, that have a the OH group of their alanine carboxyl group pointing towards the π-system of the phenyl ring are significantly more stable than all other conformers, showing that the excess negative charge localized on the ring is stabilized by the hydrogen bond. However, for the NPNPSA anion shown in Figure 11 we were unable to find this type of conformer, instead the most stable valence anion conformer type has a hydrogen bond to one of the sulfonyl oxygen atoms. Clearly the attached electron has a strong influence not only on the local bonding of the group that it is attached to but also on the more delicate intermolecular-like contacts and the preferred conformation of the larger molecule as a whole.

The computed VDEs and AEAs for the low-energy conformers of NPNPSA and NPNPA are collected in Tables III and IV. The reported AEAs are "local" in the sense that the energy difference listed is the one between *corresponding* conformers of neutral and anion. It is termed "local," because it can occur with small adjustments of geometry. The local AEA is expected to be relevant for interpreting the photoelectron spectra, because only detachment resulting in small changes of geometry can have favorable Franck-Condon factors. The true AEA is of course the energy difference between

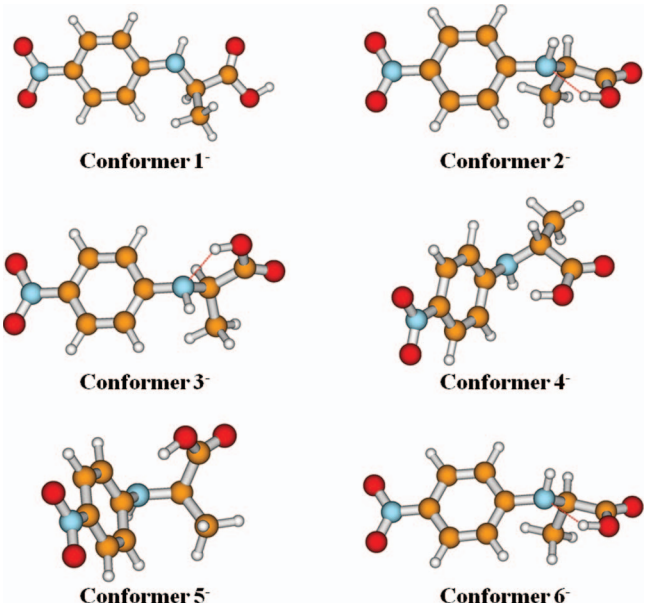

FIG. 10. The six low energy conformers of the NPNPA valence anion.

the most stable conformer of the neutral and the most stable conformer of the respective anion, but for both NPNPSA and NPNPA the true AEA is expected to have virtually zero intensity in a PES. For NPNPSA the true AEA is predicted to be 1.87 eV, yet under the assumption that the experimental anion population consists essentially of the two most stable conformers (conformers 3^- and 4^-), and taking into account a zero-point correction on the order of 0.1 eV, the calculations predict a local AEA on the order of 1.9 eV and a VDE of 2.3 eV.

For NPNPA the situation is less clear cut. The local AEAs of the anion conformers are listed in Table IV. Three or four conformers (conformers 2^-, 3^-, 4^-, and 6^-,) could have significant abundance in an experimental anion population. These four conformers have significantly different AEAs and VDEs; therefore, substantial inhomogeneous broadening may be expected for the photoelectron spectrum of NPNPA, if one were obtained. The predicted range for the local AEA is 0.9–1.1 eV and for the VDE is 1.3–1.4 eV with the true AEA

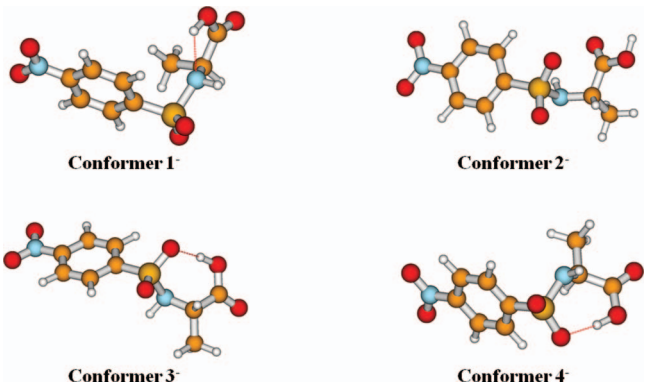

FIG. 11. The four low energy conformers of the NPNPSA valence anion.

TABLE III. The calculated adiabatic electron affinities (AEA) and vertical detachment energies (VDE) of the low-lying energy NPNPSA valence anion conformers, using OLYP/ma-Def2-TZVP energy differences at the M06-2X/aug-cc-pVDZ minimal-energy geometries

Conformer (anion)	AEA (eV)	VDE (eV)
1^-	2.02	2.32
2^-	1.66	2.06
3^-	2.06	2.42
4^-	2.01	2.40

calculated to be 1.08 eV (energy difference between neutral conformer 1 and anion conformer 3^-).

V. CONCLUSION

The gas phase negative ion properties of two extended molecular structures-NPNPSA and NPNPA were examined both experimentally and theoretically. Conformers 1 and 3 of NPNPA and conformer 2 of NPNPSA are predicted to support a dipole bound state (see Figure 12). These were not observed experimentally because the ion source was not appropriate for creating dipole bound anions.[33] The calculated adiabatic electron affinity was in good agreement with the experimentally measured AEA of 1.7 ± 0.1 eV for NPNPSA. This value is almost twice that for nitrobenzene (1.00 eV[1]) showing the effect of the extended system. Also, the vertical detachment energy of the NPNPSA negative ion was measured to be approximately 2.3 ± 0.1 eV, which compares quite well with the calculated VDE of 2.3 eV. The experimental and theoretical agreement for (*S*)- and (*R*)-NPNPSA as well as that of nitrobenzene provide confidence for at least the predicted AEA and VDE of the NPNPA conformers.

Every observed fragmentation pathway of $(NPNSA\text{-}H)^-$ and $(NPNPA\text{-}H)^-$ anions, excluding the very weak channels of the NO_2 anion and a deprotonated nitrosobenzene at the para-position, contained the nitrobenzene moiety even though the anions were created via a deprotonation of a carboxylic acid. This was due to the stabilizing effect due to delocalization of the excess electron on the π orbitals of the nitrobenzene molecule. Estimates of the energy thresholds for dissociation into the various ion channels are presented but multiple collisions are present and that limits the accuracy of the estimations. The thresholds are lowered by collision induced vibrational excitation (heating) of the $(NPNPSA\text{-}H)^-$ and $(NPNPA\text{-}H)^-$ anions.

TABLE IV. The calculated local adiabatic electron affinities (AEA) and vertical detachment energies (VDE) of the low-lying energy NPNPA anion conformers, using OLYP/ma-Def2-TZVP energy differences at the M06-2X/aug-cc-pVDZ minimal-energy geometries.

Conformer (anion)	AEA (eV)	VDE (eV)
1^-	0.69	0.97
2^-	1.24	1.52
3^-	1.06	1.41
4^-	1.06	1.40
5^-	1.07	1.64
6^-	1.12	1.52

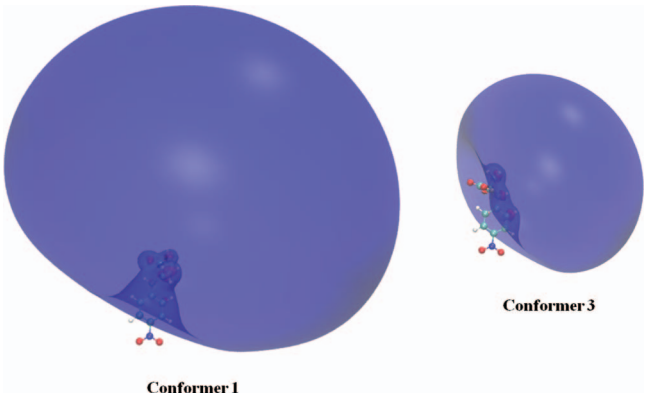

FIG. 12. Dipole-bound orbitals of NPNPA conformers 1 and 3. The isosurfaces shown enclose 75% of the electron density that corresponds to isocontour values of 0.0010 and 0.0022, respectively. The associated electron binding energies are listed in Table S7 of the supplementary material.[33]

ACKNOWLEDGMENTS

Parts of this research are based on work supported by the National Science Foundation under Grant Nos. CHE-1111693 (K.H.B.), CHE-0848487 (R.N.C.), and CHE-0954297 (M.D.B.). Acknowledgment is made to the Donors of the American Chemical Society Petroleum Research Fund for partial support of this research.

[1]C. Desfrancois, V. Periquet, S. A. Lyapustina, T. P. Lippa, D. W. Robinson, K. H. Bowen, H. Nonaka, and R. N. Compton, J. Chem. Phys. **111**, 4569 (1999).
[2]C. J. Noren, S. J. Anthony-Cahill, M. C. Griffith, and P. G. Schultz, Science **244**, 182 (1989).
[3]D. B. F. Johnson, J. Xu, Z. Shen, J. K. Takimoto, M. D. Schultz, R. J. Schmitz, Z. Xiang, J. R. Ecker, S. P. Briggs, and L. Wang, Nat. Chem. Biol. **7**, 779 (2011).
[4]J. Xieand and P. G. Schultz, Nat. Rev. Mol. Cell Biol. **7**, 775 (2006).
[5]D. A. Dougherty, Curr. Opin. Chem. Biol. **4**, 645 (2000).
[6]S. Wen, K. Nanda, Y. Huang, and G. J. O. Beran, Phys. Chem. Chem. Phys. **14**, 7578 (2012).
[7]M. L. Di Gioia, A. Leggio, A. Le Pera, A. Liguori, and C. Siciliano, J. Org. Chem. **70**, 10494 (2005).
[8]T. Kowalik-Jankowska, H. Kozlowski, K. Pawelczak, and M. Makowski, J. Chem. Soc. Dalton Trans. **1995**, 2729.
[9]P. L. Meo, F. D'Anna, M. Gruttadauria, S. Riela, and R. Noto, Tetrahedron **60**, 9099 (2004).
[10]D. M. Neumark, K. R. Lykke, T. Andersen, and W. C. Lineberger, Phys. Rev. A **32**, 1890 (1985).
[11]B. H. Smith, A. Buonaugurio, J. Chen, E. Collins, K. H. Bowen, R. N. Compton, and T. Sommerfield, J. Chem. Phys. **138**, 234304 (2013).
[12]T. H. Dunning, J. Chem. Phys. **90**, 1007 (1989).
[13]R. A. Kendall, T. H. Dunning, and R. J. Harrison, J. Chem. Phys. **96**, 6796 (1992).
[14]F. Weigend and R. Ahlrichs, Phys. Chem. Chem. Phys. **7**, 3297 (2005).
[15]E. Papajak and D. G. Truhlar, J. Chem. Theory Comput. **6**, 597 (2010).
[16]Y. Zhao and D. G. Truhlar, J. Phys. Chem. A **110**, 5121 (2006).
[17]M. Nooijen and R. J. Bartlett, J. Chem. Phys. **102**, 3629 (1995).
[18]J. F. Stanton and J. Gauss, J. Chem. Phys. **103**, 1064 (1995).
[19]J. P. Perdew, K. Burke, and M. Ernzerhof, Phys. Rev. Lett. **77**, 3865 (1996).
[20]A. D. Becke, Phys. Rev. A **38**, 3098 (1988).
[21]C. Lee, W. Yang, and R. G. Parr, Phys. Rev. B **37**, 785 (1988).
[22]A. D. Becke, J. Chem. Phys. **98**, 5648 (1993).
[23]A. J. Cohen and N. C. Handy, Mol. Phys. **99**, 607 (2001).
[24]J. Tao, J. P. Perdew, V. N. Staroverov, and G. E. Scuseria, Phys. Rev. Lett. **91**, 146401 (2003).
[25]M. J. Frisch, G. W. Trucks, H. B. Schlegel *et al.*, GAUSSIAN 09, Revision B.1, Gaussian, Inc., Wallingford, CT, 2009.
[26]ORCA, version 2.8.0, written by F. Neese, with contributions from U. Becker, D. Ganiouchine, S. Koßmann, T. Petrenko, C. Riplinger, and F. Wennmohs, see http://www.thch.uni-bonn.de/tc/orca/.
[27]CFOUR, version 1, J. F. Stanton, J. Gauss, M. E. Harding, P. G. Szalay, with contributions from A. A. Auer, R. J. Bartlett, U. Benedikt, C. Berger, D. E. Bernholdt, Y. J. Bomble, L. Cheng, O. Christiansen, M. Heckert, O. Heun, C. Huber, T.-C. Jagau, D. Jonsson, J. Jusélius, K. Klein, W. J. Lauderdale, D. A. Matthews, T. Metzroth, L. A. Mück, D. P. O'Neill, D. R. Price, E. Prochnow, C. Puzzarini, K. Ruud, F. Schiffmann, W. Schwalbach, S. Stopkowicz, A. Tajti, J. Vázquez, F. Wang, J. D. Watts and the integral packages MOLECULE (J. Almlöf and P. R. Taylor), PROPS (P. R. Taylor), ABACUS (T. Helgaker, H. J. Aa. Jensen, P. Jørgensen, and J. Olsen), and ECP routines by A. V. Mitin and C. van Wüllen. For the current version, see http://www.cfour.de.
[28]H. Y. Afeefy, J. F. Liebman, and S. E. Stein, *NIST Chemistry WebBook, NIST Standard Reference Database Number 69*, edited by P. Linstrom and W. G. Mallard (National Institute of Standards and Technology, Gaithersburg, MD, 2010).
[29]Z. Wang, C. E. C. A. Hop, M.-S. Kim, S.-E. W. Huskey, T. A. Baillie, and Z. Guan, Rapid Commun. Mass Spectrom. **17**, 81 (2003).
[30]M. Karni and A. Mandelbaum, Org. Mass Spectrom. **15**, 53 (1980).
[31]K. Levsen, H.-M. Schiebel, J. K. Terlouw, K. J. Jobst, M. Elend, A. Preiss, H. Thiele, and A. Ingendoh, J. Mass Spectrom. **42**, 1024 (2007).
[32]C. D. Cooper and R. N. Compton, Chem. Phys. Lett. **14**, 29 (1972).
[33]See supplementary material at http://dx.doi.org/10.1063/1.4834675 for additional CID results, additional calculations, and discussion on the dipole-bound anions of nitrobenzene, NPNPSA, and NPNPA.